Journal of Hazardous Materials 168 (2009) 276–281

Contents lists available at ScienceDirect

Journal of Hazardous Materials

journal homepage: www.elsevier.com/locate/jhazmat

Effect of TiO_2/adsorbent hybrid photocatalysts for toluene decomposition in gas phase

Jinhan Mo, Yinping Zhang*, Qiujian Xu, Rui Yang

Department of Building Science, Tsinghua University, Beijing 100084, PR China

ARTICLE INFO

Article history:
Received 31 October 2008
Received in revised form 6 February 2009
Accepted 6 February 2009
Available online 20 February 2009

Keywords:
Absorbents
Hybrid phtotocatalysts
Photocatalytic oxidation (PCO)
Langmuir–Hinshelwood kinetics
Toluene

ABSTRACT

12 hybrid photocatalysts consisting of titania (TiO_2) and an adsorbent such as mordenite were investigated for the photocatalytic decomposition of toluene, a major indoor contaminant in indoor air. The highest decomposition rate was obtained with the use of mordenite and silicon dioxide (SiO_2) as additives to TiO_2. The photocatalytic activities of hybrid photocatalysts in decomposing toluene are 1.33 times as high as pure P25 at the net weight loading of 0.49 mg/cm^2 under the test condition. Scanning electron microscopy (SEM) images confirmed that the hybrid photocatalyst films were very porously distributed; TiO_2 was adsorbed on the surface of mordenite and SiO_2, increasing the reaction area of TiO_2. The unimolecular Langmuir–Hishelwood model and mass-transfer-based (MTB) method were used to evaluate the reaction coefficients and adsorption equilibrium coefficients of hybrid photocatalysts. It is evidenced that the reaction areas of two hybrid photocatalysts were 1.52 and 1.64 times larger than that of P25, respectively, which is the major reason to make the high removal efficiency of toluene.

1. Introduction

In the past decades, buildings have been sealed more tightly to reduce the energy consumption. Meanwhile, synthetic building materials and furnishings, which emit volatile organic compounds (VOCs), were widely used in the urban buildings. These situations made the indoor VOC concentrations being higher than the level permitted by the standards (e.g., the Chinese National Standard GB9671 [1]). Those may cause general symptoms, such as headache; eye, nose or throat irritations; dry cough; dizziness and nausea; difficulty in concentrating; and tiredness [2–5]. Those may also do great harm to respiratory system, cardiovascular system and nervous system of human beings [6].

Developing effective technology for a sustainable environment aiming at removing VOCs quickly and economically is now a recognized goal of many governmental and industrial organizations and researchers in the related fields. Photocatalytic oxidation (PCO) by employing UV radiation is an innovative and promising approach that may meet such demand. When a semiconductor material such as nanometer titania (TiO_2) particles is illuminated by photons of greater energy than their band-gap energies, the material absorbs the photons. The electrons in the valence band of the material are excited into the conduction band and leave electron holes in the valence band. The components of this activated pair, when transferred across the interface, are capable of reducing and oxidizing a surface-adsorbed organic compound. Studies have shown that gas–solid photocatalysis may decompose a wide variety of VOCs, including typical indoor contaminant such as acetone, toluene, formaldehyde and benzene [7–9]. TiO_2 is a commonly used photocatalyst because of its high photoactivity and good stability [10]. Titania is normally loaded on the carrier surface as a thin film on which the photocatalytic reaction takes place. However, TiO_2 exhibits low adsorption ability, especially for non-polar substances due to its polar structure [11], which restricts the PCO reaction. Some researchers have found that mixing some adsorbents with nanometer TiO_2 can increase the photocatalytic reaction effectiveness in aqueous system [12–15]. Normally, it was thought that the adsorbents would absorb the compounds on the adsorbent support. Then a high concentration environment of the compounds was formed around the loaded TiO_2, resulting in an increase in the photoreaction rate. However, few have investigated this phenomenon in gas-phase systems. Yoneyama and Torimoto [16] used various adsorbents, such as zeolite, alumina, silica, mordenite, ferrierite, and activated carbon, as the support of TiO_2 and showed that the hybrid photocatalysts were effective in achieving high decomposition rates of propionaldehyde in air. The mordenite was the best among the tested adsorbents. They also found that the best weight fraction of doping mordenite with TiO_2 was 47%. However, they got this result under static experimental condition, which is not similar to normal once-through air cleaning process in indoor environment. Moreover, propionaldehyde is not a typical indoor air contaminant.

* Corresponding author. Tel.: +86 10 6277 2518; fax: +86 10 6277 3461.
E-mail address: zhangyp@mail.tsinghua.edu.cn (Y. Zhang).

0304-3894/$ – see front matter © 2009 Elsevier B.V. All rights reserved.
doi:10.1016/j.jhazmat.2009.02.033

Nomenclature

C_{in}	average inlet concentration (ppm)
C_{out}	average outlet concentration (ppm)
C_s	gas-phase concentration close to the reaction surface (ppm)
r	average decomposition rate (ppm m/s)
k	reaction coefficient (ppm m/s)
K_{ad}	adsorption equilibrium coefficient (ppm^{-1})
A_r	reaction surface area (m^2)
r'	equivalent reaction rate (ppm m/s)
k'	equivalent reaction coefficient (ppm m/s)
A'_r	projection area of reaction surface (m^2)
n	the ratio between reaction surface area and projection area
G	volumetric airflow rate (m^3/s)

In the present study, we used a glass-plate photoreactor to investigate the effect of applying TiO_2/adsorbent hybrid photocatalysts to remove low concentration toluene (ppmv level) which is a major indoor contaminant [17] for common air-conditioned space. Optimal net weight loading and mixing weight ratio of P25 and adsorbents were studied and obtained. The unimolecular Langmuir–Hishelwood (L–H) model and mass-transfer-based (MTB) method were used to evaluate the reaction coefficients and adsorption equilibrium coefficients of two hybrid photocatalysts. The reason why the hybrid photocatalysts had higher performance than pure TiO_2 was discussed.

2. Experimental

2.1. Film preparation

Degussa P25 titania is a kind of widely used nanometer photocatalyst [16,18] with a primary particle diameter of 30 nm, 50 m^2/g specific surface area, a crystal distribution of 70% anatase and 30% rutile. 12 commercial adsorbents (Table 1) were mixed with P25, respectively, at the specific weight ratios. The hybrid photocatalyst film was deposited on the glass plate with dimensions of 90.0 mm in length, 4.0 mm in height and 25.0 mm in width by dipped-coating method [19]. Before the process, the glass plate was washed in 10 wt.% NaOH solution and distilled water by sequence, and then dried in oven at 70 °C until the glass surface was dry. The solution was 1.25 wt.% of the hybrid photocatalyst or pure P25 in absolute ethanol. The film was prepared by dipping the glass plate in the dipped-coating several times, air drying between dipping, and then drying in oven at 70 °C for 2 min. This process was repeated until a specific net weight loading of material (per side) was achieved on the glass plate.

Table 1
Physical parameters of various materials.

Symbol	Material	Particle size	Specific surface (m^2/g)
P25	Degussa P25 titania	30 nm	50
AZ	Artifical zeolite	<4 μm	13
CR	Clinoptilolite (R)	325 mesh	0.65–0.70
CY	Clinoptilolite (Y)	325 mesh	0.65–0.70
CW	Clinoptilolite (W)	280–290 mesh	0.57
M	Mordenite	12–16 μm	250–300
S1	SiO_2 (SD-400L)	1 μm	260–320
S2	SiO_2 (SD-520)	2 μm	300–350
S3	SiO_2 (SD-520L)	2 μm	300–350
A	Alumina	10 μm	250
Z1	ZSM-5-25H molecular sieve		
Z2	ZSM-5-38H molecular sieve	2–4 μm	342–360
Z3	ZSM-5-50H molecular sieve		

2.2. Glass-plate photoreactor

The decomposing effect of toluene was measured in a glass-plate photoreactor (Fig. 1). Two parallel germicidal lamps (254 nm peak intensity, Philips Hg-Lamp, TUV 15W G15T8 UV-C, made in Holland) provided UV light for the photoreactor. Adjusting the distance between the light and the photoreactor varied the light intensity. The light intensity at the reaction surface was measured using a UV power meter (HANDY 00000176, made in China). Synthetic air (mixture of high-purity nitrogen and oxygen with volume ratio 79:21) was supplied from a compressed cylinder. The air passed through a filter and was then divided into two streams. One stream passed through a flow meter while the other passed through a humidifier to control the tested air on the desired humidity level. Toluene was mixed with the synthetic air and then the mixed gas was supplied through a mass flow controller to the reactor. The photocatalyst-coated glass plates were placed in a well (25.0 mm wide, 380.0 mm long and 4.0 mm deep) made of stainless steel and covered with a quartz window (its transmittance at 254 nm wavelength is 0.80). The space between the photocatalyst-coated glass plate and the quartz window was the flow section of 25.0 mm wide and 2.0 mm high.

INNOVA photoacoustic multi-gas monitor 1312 and multipoint sampler and doser 1303 were used to measure the inlet and outlet concentrations of the reactor: water vapor, carbon dioxide, carbon monoxide and toluene. Four copper–constantan thermocouples were installed at the photoreactor inlet, outlet and inside, respectively. A data logger recorded the temperature. Table 2 lists the uncertainly of the measured parameters. All experiments were performed at room temperature of 25.0–27.0 °C. The relative humidity (RH) was set to a common air conditioning level of about 47%. The total air volumetric flow rate was 4.00 L/min, which formed a laminar flow with Reynolds number (based on the 25.0 mm by 2.0 mm flow cross-sectional area) of 330 in the reactor. The UV light intensity at the glass-plate surface was 1.64 mW/cm^2. Three pieces of same-coated glass plates were placed in series in the photoreactor. The other glass plate (90.0 mm long, 25.0 mm wide and 4.0 mm thick) without photocatalyst was placed in front of the coated glass plates to make the reaction part being in the fully developed region of laminar flow. Each experiment was repeated under the same experiment condition.

2.3. Test procedure

The procedure for all the experiments was as follows: (1) airflow was started; (2) after the photoreactor inlet and outlet humidity readings were steady and equal, the toluene was introduced; (3) when the photoreactor inlet and outlet toluene concentrations were approximately equal, the UV lamps were turned on; (4) after the inlet and outlet toluene levels again reached steady state, the UV lamps were turned off and the toluene flow was stopped; and (5) the photoreactor was flushed with the synthetic air for 15 min, and then airflow was stopped. Normally, it took about 3 h to finish the whole procedures.

2.4. Data analysis and characterization

For the data measured by the glass-plate photoreactor, the single-pass removal efficiency, ε was used [20,21]:

$$\varepsilon = \frac{C_{in} - C_{out}}{C_{in}} \quad (1)$$

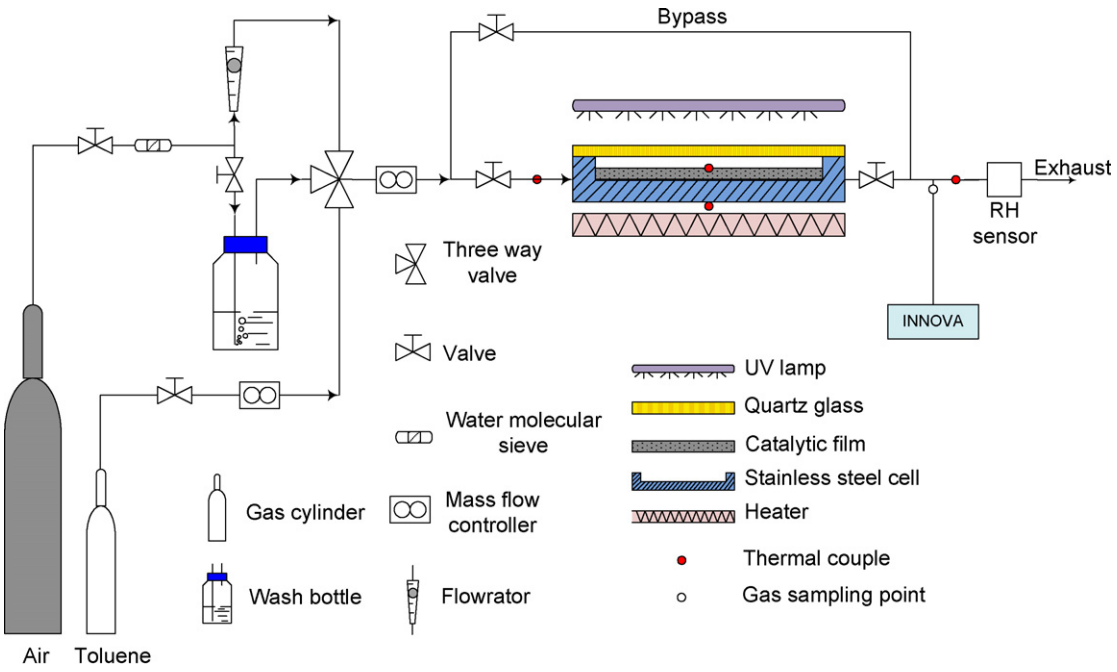

Fig. 1. Schematic of the experimental system, including the gas preparation part and UV–PCO reaction cell.

where C_{in} is the average toluene concentration at the inlet under the steady state when the UV lamps are lighting. C_{out} is the corresponding value at the outlet. Normally, the average decomposition rate of toluene, r followed the unimolecular type L–H model [22–24]:

$$r = k\frac{K_{ad}C_s}{1 + K_{ad}C_s} \quad (2)$$

where k is the reaction coefficient (dependent on temperature, UV intensity and photocatalyst, etc.); K_{ad} is adsorption equilibrium coefficient and C_s is the gas-phase concentration of toluene close to the reaction surface. K_{ad} and k are the kinetic parameters to evaluate the adsorption and photoreaction performance of photocatalyst, respectively. In this study, a least-squares optimization was performed to obtain K_{ad} and k by fitting the experimental data. Based on Eq. (2), the reaction rate, r and C_s are usually used as the necessary kinetic data for data-fitting. r is also calculated as follows [25]:

$$r = \frac{G(C_{in} - C_{out})}{A_r} \quad (3)$$

where G is the volumetric airflow rate and A_r is reaction surface area. Normally, the area of reaction surface is close to its projection area [25,26], that is, $A_r = A'_r$. If not, it is assumed that A_r is n times larger than A'_r, that is, $A_r = nA'_r$. Define the equivalent reaction rate and reaction coefficient as $r' = nr$ and $k' = nk$. Eq. (2) can be rewritten as

$$r' = k'\frac{K_{ad}C_s}{1 + K_{ad}C_s} \quad (4)$$

C_s can be obtained by MTB developed by Yang et al. [26]. The experiments were all under the reaction controlled conditions (More details were shown in the Supplementary Material.). All analyses used a 95% confidence level.

Scanning electron microscopy (SEM) observation was performed using a Chinese Academy of Sciences Tech. Plant instrument (KYKY-2800).

Table 2
Measurement uncertainty of measured parameters.

Measured parameters	Measurement uncertainty
Inlet and outlet toluene concentration	$\pm[(0.012 \times 3/\text{concentration})^2 + 0.02^2]^{0.5}$
Inlet and outlet water vapor concentration	±2%
Airflow rate	±1%
UV light intensity	±5%
Temperature	±0.2 °C
Film weight	±1 mg

3. Results

3.1. Photoactivity of various hybrid photocatalysts

Fig. 2 shows the toluene decomposition efficiencies of 12 hybrid photocatalysts (mixing adsorbents with P25, weight ratio of 1:1)

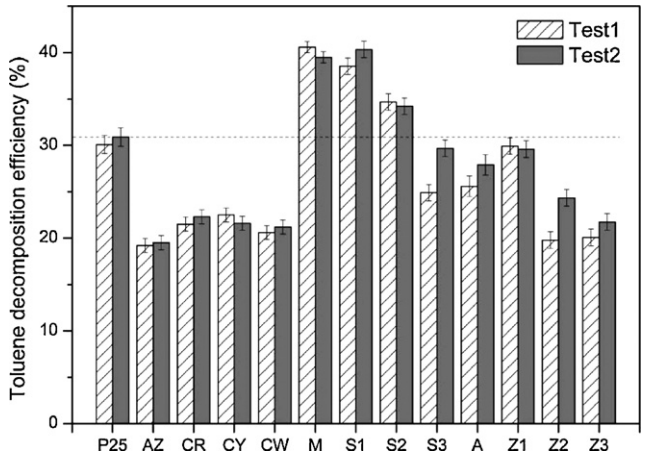

Fig. 2. Comparison of 12 hybrid photocatalysts (mixing adsorbents with P25, weight ratio of 1:1, net weight loading of 0.49 mg/cm^2) and pure P25 on the removal efficiency of toluene: 2.5 ppm inlet toluene; 4.00 L/min airflow rate; 47% relative humidity; 25.0–27.0 °C air temperature; 1.64 mW/cm^2 UV light intensity.

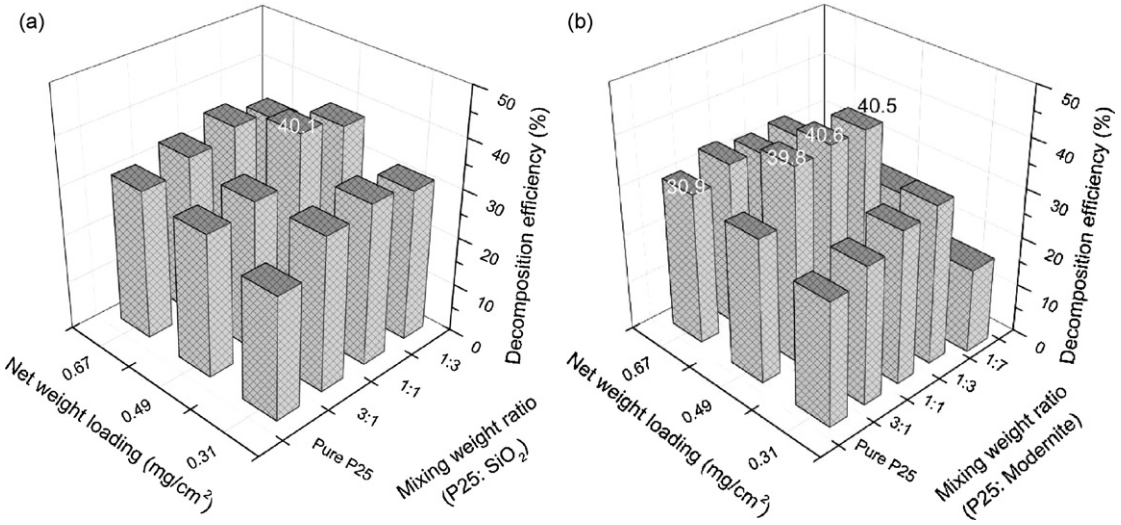

Fig. 3. Effect of different weight ratios and net weight loadings of hybrid photocatalysts ((a) S1; (b) M) on the removal efficiency of toluene: 2.5 ppmv inlet toluene; 4.00 L/min airflow rate; 47% relative humidity; 25.0–27.0 °C air temperature; 1.64 mW/cm^2 UV light intensity.

and pure P25 in two individual tests with inlet toluene concentration of 2.5 ppm. The net weight loading of glass plates were all 0.49 mg/cm^2. It is noticed that the toluene removal performance of most hybrid photocatalysts decreased compared with pure P25. It may be due to three reasons. Firstly, the adsorbents have too low adsorption constant, such as A, AZ, CR, CY and CW in this study. They have lower specific surfaces than pure P25. Secondly, the adsorbents have high adsorption constant. Yoneyama and Torimoto [16] found that the adsorbents having high adsorption constants such as activated carbon would retard the diffusion of the adsorbed pollutant to the reaction surface and decrease the decomposition rate. In this study, adsorbents Z1–Z3 have very high specific surfaces. Toluene may be strongly adsorbed on the surfaces of Z1–Z3, but not P25. Thirdly, the coverage of adsorbents reduces the reaction area.

However, there were significant enhancements of removal efficiency of P25 doped with modernite (M) and SiO_2 (S1 and S2). Compared with pure P25, the toluene removal efficiencies of samples M and S1 were improved from 30% to 40%. This result agrees with the investigation of Yoneyama and Torimoto [16], who found mordenite was the best adsorbent as the support for TiO_2. The major reaction products of toluene were CO_2 and CO (The results were shown in the Supplementary Material.).

3.2. Effect of weight ratios and net weight loading

Fig. 3 shows the variation of removal efficiency versus weight ratios and weight loading of S1 and M. For sample S1, the removal efficiency decreased at small and big amount of SiO_2 (Fig. 3(a)). The optimal toluene removal efficiency was achieved at the weight ratio of P25:SiO_2 = 1:1. There was significant difference between the weight loading of 0.31 and 0.49 mg/cm^2, while 0.49 mg/cm^2 was a little better than 0.64 mg/cm^2 (Fig. 3(a)). But the difference between 0.31 and 0.64 mg/cm^2 was slight. Thus the best loading for sample S1 was 0.49 mg/cm^2. From Fig. 3(b), it is seen that the removal efficiency decreased with increasing the amount of mordenite. However, there is no significant difference of ε among the weight ratios from 3:1 to 1:3. All of them retained high removal efficiency about 40%. The similar influence of net weight loading was also observed on sample M (Fig. 3(b)) as S1. The best loading for sample M was 0.49 mg/cm^2. The similar result was reported in aqueous system by Takeda et al. [12]. It was thought that the UV light would transmit the coating under low weight loading condition, resulting in the low decomposition efficiency. Takeda et al. [12] also observed that there was an optimum weight loading, beyond which a decreasing tendency of decomposition efficiency appeared. It resulted from the decrease of the fraction of photo-excited TiO_2 in the coating film [12]. However, the related researches were rarely presented in the field of gas system.

3.3. Kinetic parameters of hybrid photocatalysts

Focusing on the sample M (weight ratio of P25:mordenite = 1:3; weight loading of 0.49 mg/cm^2) and S1 (weight ratio of P25:SiO_2 = 1:1; weight loading of 0.49 mg/cm^2), the influence of inlet toluene concentration is given in Fig. 4. The experiment was performed with different inlet toluene concentrations in the range of 0–4.5 ppm. The single-pass removal efficiency, ε reduced with the increase of toluene concentration. The shapes of these curves are characteristic of a unimolecular reaction. The samples S1 and M both kept higher removal efficiencies than that of pure P25, while the performance of S1 is slightly better than that of M under various C_{in}.

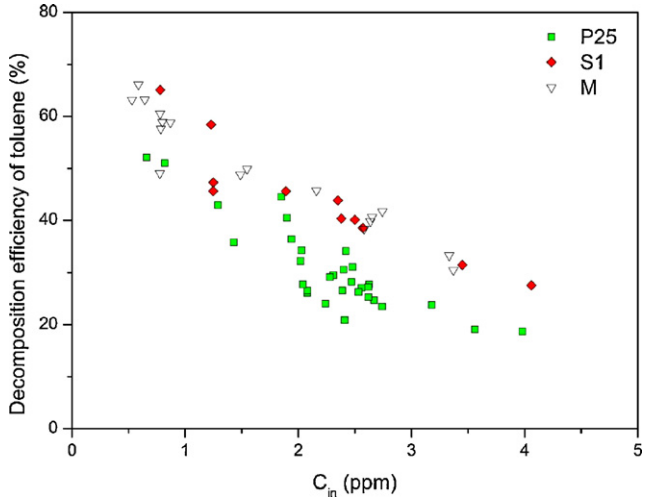

Fig. 4. Removal efficiencies of toluene versus inlet toluene concentrations: 4.00 L/min airflow rate; 47% relative humidity; 25.0–27.0 °C air temperature; 1.64 mW/cm^2 UV light intensity.

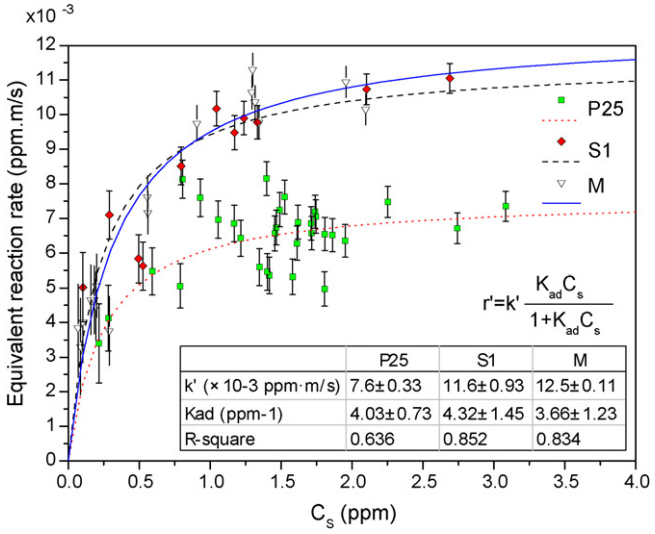

Fig. 5. Equivalent reaction rate versus C_s. The lines mean the calculated results by Eq. (4).

By representing r' versus C_s, the equivalent L–H reaction coefficient k' and the adsorption equilibrium coefficient K_{ad} of pure P25, S1 and M were evaluated and compared with that of pure P25 in Fig. 5. The resulting correspondence between the L–H correlation and the experimental data shows good fitting behavior (Fig. 5). The important observation is that the values of k' of S1 and M are both much larger than the value of pure P25. However, the values of K_{ad} are quite insensitive to the loading of SiO_2 and mordenite.

3.4. SEM analysis

Fig. 6 shows the SEM morphology of pure P25, M and S1 at the net weight loading of 0.49 mg/cm^2. Dense structure with uniformly distributed film was observed in pure P25, while the surface of samples M and S1 were very coarse (Fig. 6(a–c)). With larger magnification times, it is obvious that the mordenite particles were almost covered by nanometer P25 (Fig. 6(e)), which formed the porous surface (Fig. 6(b)). Although, the structures of samples M and S1 were both porous, the SiO_2 particles staggered with P25 on the surface (Fig. 6(f)) and only part of SiO_2 particles was covered by P25.

4. Discussion

In 12 hybrid pohotocatalysts, samples M and S1 were found to have highest removal efficiencies of toluene. Generally, the loaded adsorbents were thought to increase the adsorbability of photocatalyst [11,16]. The rate of chemical reactions is determined by the concentration of the chemical compounds [16]. The adsorbents would adsorb the compounds on the adsorbent support. Then a high concentration environment of the compounds was formed around the loaded TiO_2, resulting in an increase in the removal efficiency. In this study, two types of hybrid photocatalysts (S1 and M) show higher photocatalyst decomposition performance of toluene than pure P25. However, the adsorption equilibrium coefficients K_{ad} of these two hybrid photocatalysts standing for their adsorbability were not found to be increased. On the contrary, K_{ad} of sample M was smaller than that of pure P25, which may result from the data-fitting error (see the table in Fig. 5). It is believable that the adsorbabilities of these three samples are almost the same. It evidenced that the decomposition rate was not contributed by increasing the adsorbability, which did not agree with the results found in the earlier study [16]. Thus, the increase of k' determined the high decomposition performance based on Eq. (4).

From the previous definition, the ratio of k' and A_r between S1 and P25 are the following:

$$n_{S1-P25} = \frac{k'_{S1}}{k'_{P25}} = \frac{n_{S1}k_{S1}}{n_{P25}k_{P25}} = \frac{A_{r,S1}/A'_r}{A_{r,P25}/A'_r}\frac{k_{S1}}{k_{P25}} = \frac{A_{r,S1}}{A_{r,P25}}\frac{k_{S1}}{k_{P25}} \quad (5)$$

where the subscript S1–P25 stands for the ratio between S1 and P25. Because the adsorbent has no photocatalytic response under UV irradiation, the reaction rate constant (or reaction coefficient) k should not change after the addition of S1, that is, k_{S1} is equal to k_{P25}. Thus, the ratio of reaction area between S1 and P25 is equal to the value of n_{S1-P25}, which is calculated as 1.52 based on Eq. (5). In a similar way, n_{M-P25} is calculated as 1.64. It means the reaction

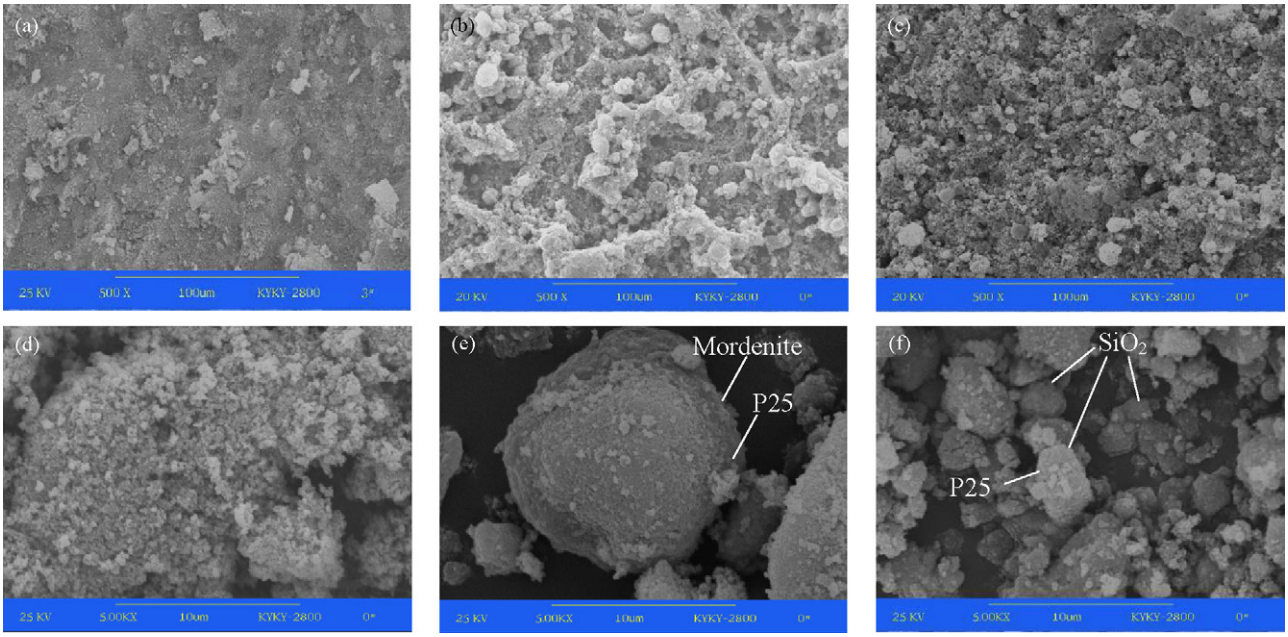

Fig. 6. SEM morphology of various hybrid photocatalysts at net weight loading of 0.49 mg/cm^2. (a) Pure P25; (b) P25:mordenite = 1:3; (c) P25:SiO_2 = 1:1. The magnification times of (d), (e) and (f) are 10 times higher than those of (a), (b) and (c), respectively.

areas of samples S1 and M are 1.52 and 1.64 times larger than that of P25, respectively.

Fig. 6 shows the reason why the hybrid photocatalysts obtained large reaction surface. The big particle sizes of mordenite and SiO_2 (Table 1) made them to be the supports of P25 (Fig. 6). Mordenite and SiO_2 particles adsorbed abundant nanoscale P25 particles during dipped-coating process and then were coated on the surface of glass plates. The porous coatings supported larger reaction surface than P25 coating. For sample S1, P25 only occupied part of SiO_2 particles, while the mordenite particles were almost covered by P25. Thus, sample S1 shows slightly larger K_{ad} value due to its stronger adsorbability than P25. But sample M provides more reaction surface than S1. However, the reaction surface was simultaneity occupied by P25 and adsorbents at large weight ratio (for S1, 1:3 and for M, 1:7) (Fig. 3). It decreased the reaction area and restrained ε. In summary, the reaction surface plays a leading role in increasing the removal efficiencies of toluene.

5. Conclusions

12 TiO_2/adsorbent hybrid photocatalysts were prepared by dipped-coating method. A glass-plate photoreactor was used to investigate the effect of these hybrid photocatalysts on the photocatalytic reaction efficiencies for decomposing gas-phase toluene. The highest decomposition rate was obtained with the use of silicon dioxide (SiO_2) and mordenite as additives for TiO_2. Optimal net weight loading and mixing weight ratio of P25 and adsorbents were studied and obtained. The photocatalytic activities of hybrid photocatalysts in degradation 2.5 ppm toluene are 1.33 times as high as pure P25 at the net weight loading of 0.49 mg/cm^2 under the test condition. Unimolecular L–H model and MTB method were used to evaluate the reaction coefficient and adsorption equilibrium coefficient of hybrid photocatalysts S1 and M. It evidenced that the reaction areas of samples S1 and M are 1.52 and 1.64 times larger than that of P25, respectively, which is the major reason to make the high removal efficiency of toluene. The study indicates that building a porous reaction surface such as adding adsorbents or porous supporter is a novel way to increase the performance of PCO material for removing indoor VOCs.

Acknowledgements

We gratefully acknowledge the support of National Nature Science Foundation of China (grant nos. 50436040 and 50725620) and National 11th Five-Year Plan of Dept. of Science, China (grant no. 2006BAJ02A08).

Appendix A. Supplementary data

Supplementary data associated with this article can be found, in the online version, at doi:10.1016/j.jhazmat.2009.02.033.

References

[1] Chinese National Standard, GB9671-1996: Hygienic Standard for Reception Room in Hospital, 1996.
[2] World Health Organization, Indoor air quality: organic pollutants. Report on a WHO meeting, EURO Report and Studies, 1989, pp. 1–70.
[3] Y.M. Kim, S. Harrad, R.M. Harrison, Concentrations and sources of VOCs in urban domestic and public microenvironments, Environ. Sci. Technol. 35 (2001) 997–1004.
[4] USEPA, Reducing Risk: Setting Priorities and Strategies for Environmental Protection, U.S. Environmental Protection Agency, 1990.
[5] P. Wolkoff, P.A. Clausen, B. Jensen, G.D. Nielsen, C.K. Wilkins, Are we measuring the relevant indoor pollutants? Indoor Air 7 (1997) 92–106.
[6] L. Molhave, Sick buildings and other buildings with indoor climate problems, Environ. Int. 15 (1989) 65–74.
[7] J.L. Shie, C.H. Lee, C.S. Chiou, C.T. Chang, C.C. Chang, C.Y. Chang, Photodegradation kinetics of formaldehyde using light sources of UVA, UVC and UVLED in the presence of composed silver titanium oxide photocatalyst, J. Hazard. Mater. 155 (2008) 164–172.
[8] W. Wang, L.W. Chiang, Y. Ku, Decomposition of benzene in air streams by UV/TiO_2 process, J. Hazard. Mater. 101 (2003) 133–146.
[9] D.T. Tompkins, Evaluation of photocatalytic air cleaning capability: a literature review and engineering analysis, ASHARE Research Project RP-1134, 2001.
[10] B. Ohtani, Preparing articles on photocatalysis – beyond the illusions, misconceptions, and speculation, Chem. Lett. 37 (2008) 217–229.
[11] A. Bhattacharyya, S. Kawi, M.B. Ray, Photocatalytic degradation of orange II by TiO_2 catalysts supported on adsorbents, Catal. Today 98 (2004) 431–439.
[12] N. Takeda, N. Iwata, T. Torimoto, H. Yoneyama, Influence of carbon black as an adsorbent used in TiO_2 photocatalyst films on photodegradation behaviors of propyzamide, J. Catal. 177 (1998) 240–246.
[13] T. Torimoto, Y. Okawa, N. Takeda, H. Yoneyama, Effect of activated carbon content in TiO_2-loaded activated carbon on photodegradation behaviors of dichloromethane, J. Photochem. Photobiol. A 103 (1997) 153–157.
[14] Y.M. Xu, C.H. Langford, Photoactivity of titanium dioxide supported on MCM41, zeolite X, and zeolite Y, J. Phys. Chem. B 101 (1997) 3115–3121.
[15] Y.M. Xu, W. Zheng, W.P. Liu, Enhanced photocatalytic activity of supported TiO_2: dispersing effect of SiO_2, J. Photochem. Photobiol. A 122 (1999) 57–60.
[16] H. Yoneyama, T. Torimoto, Titanium dioxide/adsorbent hybrid photocatalysts for photodestruction of organic substances of dilute concentrations, Catal. Today 58 (2000) 133–140.
[17] T. Godish (Ed.), Indoor Air Pollution Control, Lewis, Chelsea, 1989.
[18] Z.B. Wu, F. Dong, W.R. Zhao, S. Guo, Visible light induced electron transfer process over nitrogen doped TiO_2 nanocrystals prepared by oxidation of titanium nitride, J. Hazard. Mater. 157 (2008) 57–63.
[19] R. Yang, Y.P. Zhang, R.Y. Zhao, An improved model for analyzing the performance of photocatalytic oxidation reactors in removing volatile organic compounds and its application, J. Air Waste Manage. Assoc. 54 (2004) 1516–1524.
[20] S. Hager, R. Bauer, G. Kudielka, Photocatalytic oxidation of gaseous chlorinated organics over titanium dioxide, Chemosphere 41 (2000) 1219–1225.
[21] Y.P. Zhang, R. Yang, R.Y. Zhao, A model for analyzing the performance of photocatalytic air cleaner in removing volatile organic compounds, Atmos. Environ. 37 (2003) 3395–3399.
[22] J.H. Mo, Y.P. Zhang, R. Yang, Novel insight into VOC removal performance of photocatalytic oxidation reactors, Indoor Air 15 (2005) 291–300.
[23] M.L. Sauer, D.F. Ollis, Acetone oxidation in a photocatalytic monolith reactor, J. Catal. 149 (1994) 81–91.
[24] H.M. Liu, Z.W. Lian, X.J. Ye, W.F. Shangguan, Kinetic analysis of photocatalytic oxidation of gas-phase formaldehyde over titanium dioxide, Chemosphere 60 (2005) 630–635.
[25] T.N. Obee, Photooxidation of sub-parts-per-million toluene and formaldehyde levels on titania using a glass-plate reactor, Environ. Sci. Technol. 30 (1996) 3578–3584.
[26] R. Yang, Y.P. Zhang, Q.J. Xu, J.H. Mo, A mass transfer based method for measuring the reaction coefficients of a photocatalyst, Atmos. Environ. 41 (2007) 1221–1229.